Least Squares Reconstruction for Sparse Spectra: Application to Hyperpolarized ^{13}C Imaging

Y. S. Levin[1,2], D. Mayer[1], Y-F. Yen[3], R. Hurd[3], D. M. Spielman[1,2]

[1]Department of Radiology, Stanford University School of Medicine, Stanford, CA, United States, [2]Department of Electrical Engineering, Stanford University School of Engineering, Stanford, CA, United States, [3]Advanced Sciences Laboratory, GEHealthcare, Menlo Park, CA, United States

Introduction Hyperpolarization of ^{13}C has made possible the imaging of metabolism in vivo; an injected compound and its downstream metabolites can be distinguished on the basis of chemical shift (1,2) . Rapid imaging is necessary because the hyperpolarized signal decays with T_1. Although the bandwidth of the carbon spectrum is large, it is also sparse. Spectral sampling can therefore be performed below the Nyquist rate, allowing spectral peaks to alias into regions of the spectrum that contain no metabolites. Spiral CSI (spcsi) (3), which maximizes efficiency of data acquisition by varying both x and y gradients simultaneously is a technique that allows the user to take advantage of this aliasing. A conventional reconstruction (CR) of the acquired data would involve performing a 1D FFT in k_f to separate the metabolites. The resulting data, a 3D data set in k_x, k_y and frequency, are demodulated with the known frequency of each of the metabolites and then gridded. This work proposes an alternate reconstruction technique based on a least squares (LS) algorithm. The technique allows the user to include additional a priori knowledge in the reconstruction, to better choose acquisition parameters, and to minimize acquisition time.

Theory For a spectrum containing known peaks, the signal as a function of time and k-space location can be expressed as $y(k_x,k_y,t) = \Sigma_j M(k_x,k_y,\nu_j) \exp(-i2\pi\nu_j t)$, where ν_i are the known frequencies present in the spectrum. For spiral CSI in which a single k-space trajectory is repeated for a total of *M* echoes, the signal for each k_x, k_y point can be written in matrix form as $\mathbf{y} = \mathbf{Am}$, where $\mathbf{y}$ is a vector corresponding to the *M* observations of the k_x, k_y point, $\mathbf{m}$ is a vector describing the spectral components of the point, and the elements of $\mathbf{A}$ are $A_{mn} = \exp(-i2\pi\nu_n (TE_m + \tau(k_x,k_y))$. $\tau(k_x,k_y)$ is the time relative to the k-space origin. Any known information about the peaks, such as J-coupling and T_2 values, can be included in $\mathbf{A}$. LS methods can be used to solve for $\mathbf{y}$ for each k-space point, and gridding can be performed to obtain metabolic images. The user is free to choose the echo times TE_m subject to the FOV and resolution constraints of the desired images. In a technique similar to that proposed by Glover et al for fat/water separation (4) and further developed by Reeder et al for IDEAL imaging (5), $\mathbf{A}$ can be optimized. Here, condition number is used to find optimal TE values and to determine the relative benefit of acquiring additional echoes.

Procedure The reconstruction and optimization technique was investigated through simulation and phantom experiments. Simulations were performed for a set of peaks at 0,-212,-363.5,-693.7 Hz, corresponding to the resonance frequencies of $^{13}C_1$ lactate, $^{13}C_1$ alanine, $^{13}C_1$ pyruvate and ^{13}C bicarbonate, respectively. This spectrum would be expected to appear after administration of $^{13}C_1$ alanine (ala), lactate (lac), or pyruvate (pyr). This is true assuming that investigation is performed on an organ that exhibits little or no anaplerosis, in which pyr is incorporated into oxaloacetate. In practice, optimization of each TE independently is a computationally complex problem. Therefore, the TEs were constrained to be equally spaced, with the spacing $\Delta TE = 1/SW$. Because the condition number of $\mathbf{A}$ varies with τ, condition number was computed as a function of SW and time (9.1 ms for the FOV = 8 cm, in-plane resolution = 0.5 X 0.5 cm^2, single-interleaf acquisition considered here). After optimization, simulated data sets were created and images were reconstructed using least squares estimation for each k-space point. The phantom contained three tubes of 1.5M 99% enriched $^{13}C_1$ ala, lac, and a pyr-pyruvate hydrate C_1-C_2 ester (PPE). For lac on resonance at 3T, ala appears at -212 Hz, and the two PPE peaks are at -243 and -594 Hz. J-coupling patterns/constants were also measured in the phantom and incorporated into matrix $\mathbf{A}$ for improved reconstruction. Phantom measurements were performed on a GE 3T MR scanner equipped with self-shielded gradients (40 mT/m, 150 mT/m/ms). A doubly tuned (^1H-^{13}C) birdcage coil (diameter = 44mm) was used for both RF excitation and signal reception. The implemented sequence consisted of a slice(z)-selective excitation (5.4 mm) and a single-interleaf spiral readout gradient. A total of 32 echoes were acquired at SW = 109.7 Hz. 64 averages were acquired to obtain sufficient SNR in the absence of hyperpolarization. Images were reconstructed according to the LS method described above using 21 echoes and 8 echoes. The reconstructions were compared to the CR of the same data and to a separately acquired fidcsi (16 X 16 phase encodes, SW = 2000 Hz, npoints = 2048, TR = 2s) data set.

Figure 1

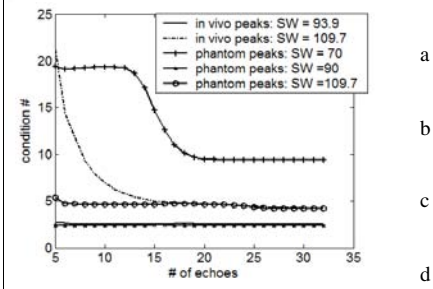

Figure 2

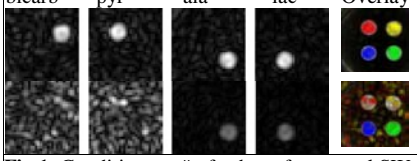

Fig 1: Condition vs. # of echoes for several SW values and for in vivo and phantom peaks.

Fig 2: Simulated individual metabolic images and color overlay for a virtual phantom containing the in vivo peaks. The top row illustrates the reconstruction for SW = 93.9 Hz. The bottom row is for 109.7 Hz.Bicarb=yellow, pyr=red, lac= blue and ala=green.

Fig 3: Top: In vitro metabolic images for each of five different reconstructions (a-e), with color overlay. ala=green, PPE=red lac=blue. Bottom: Quantitation of each metabolite in its ROI, as well as detected metabolite in the other ROI's. Thus, "L in L" refers to lac detected in the lac ROI. "P in L" refers to pyr detected in the lac ROI. All are normalized to Lactate. **a**=fidcsi data with LS recon. **b**= spcsi, 21 echoes, LS recon. **c**=spcsi, 21 echoes, CR. **d**=spcsi, 8 echoes, LS recon. **e**=spcsi, 8 echoes, CR.

Figure 3

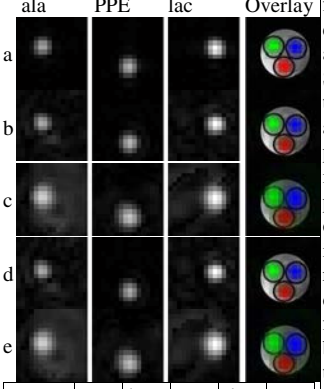

	a	b	c	d	e
L in L	1	1	1	1	1
P in L	.014	.052	.045	.045	.065
A in L	.022	.044	.217	.056	.219
A in A	.605	.651	.734	.653	.735
P in A	.014	.015	.061	.011	.068
L in A	.063	.039	.134	.035	.132
P in P	.546	.744	.756	.693	.734
A in P	.014	.118	.234	.159	.237
L in P	.018	.031	.154	.047	.165

Results Fig 1 depicts the variation of condition number with number of echoes for the first point in k-space (τ=0). Although condition varies with τ, it was empirically determined that that it does not vary enough over the 9.1 ms acquisition to warrant other choices of SW. For appropriately chosen values of SW, condition number does not improve significantly beyond a few echoes. For the in vivo peaks, SW=109.7 Hz (corresponding to the smallest possible ΔTE for a single-interleaf scan with the chosen FOV/resolution), is expected to perform poorly. SW=93.9 Hz is expected to perform much better. Fig. 2 depicts metabolic images as well as a color overlay over a grayscale image of the simulated phantom for these two SW values. Simulated SNR was set at 8 in order to demonstrate the sensitivity of image quality to SW. Fig 3 depicts metabolic images from the phantom with color overlay for each of 5 different reconstructions (see caption). The central region was cut out of the images for display. For the CR technique, four separate peaks are reconstructed, resulting in four separate metabolic images. Only one of the PPE peaks (-594 Hz) is depicted because of space considerations. The numeric table (bottom of Fig 3) quantifies the performance of each of the sequences and reconstruction techniques. An ROI of 4 pixels was chosen for each tube, and complex data values were summed; the magnitude of the result was recorded. Reported values are normalized to the lactate measurement. The performance of the LS reconstruction exceeds that of CR as seen in lower amounts of ala detected in the lac ROI, lower amounts of lac detected in the ala ROI, and lower amounts of ala detected in the pyr ROI. Additionally, performance of the LS recon with 8 echoes was comparable to performance at 21 echoes.

Conclusions: The LS reconstruction technique allows for optimization of the acquisition parameters as well as for elimination of artifacts in reconstructed images. *A priori* knowledge of anticipated resonance frequencies is required. For labeling patterns other than that described here, other spectral peaks are possible; whether they are observed depends on the rates of reaction of relevant enzymes and the T_1 of ^{13}C. For the FOV and resolution used here, our results imply that metabolic images can reliably be obtained in <85 ms, suggesting that metabolic imaging of moving organs, including the heart, is worthy of investigation.

References: (1) Ardenkjaer-Larsen JH et al. PNAS USA 2003;100:10158-10163. (2) in't Zandt R et al. Weekend Educational Syllabus, 13th ISMRM, Miami Beach; 2005. (3) Adalsteinsson E et al. MRM 1998;39:889-898. (4) Glover GH. MRM 1999;42:412-415. (5)Reeder SB et al. MRM 2004;51:35-45.